

## Improvement of Corrosion Resistance of Carbon Steel using Chemical Vapor Deposition from $\text{Cr}(\text{CO})_6$ and $\text{Mo}(\text{CO})_6$ with an ArF-Excimer Laser

Naotada OKADA, Yosuke KATSUMURA\* and Kenkichi ISHIGURE

Department of Quantum engineering and Systems Science,  
Faculty of Engineering, the University of Tokyo  
Hongo 7-3-1, Bunkyo-ku, Tokyo 113, Japan

The corrosion resistance of carbon steel has been improved by the deposition from the mixture of  $\text{Mo}(\text{CO})_6$  and  $\text{Cr}(\text{CO})_6$ , as well as from each carbonyl alone with an ArF-excimer (193nm). The corrosion resistance evaluated by multi sweep cyclic voltammetry attained by coating with the films from the mixture is higher than from  $\text{Mo}(\text{CO})_6$  alone, while lower than from  $\text{Cr}(\text{CO})_6$  alone. While the corrosion resistance increases with beam intensity monotonically over the range 4–25  $\text{MWcm}^{-2}$  for the deposition from  $\text{Mo}(\text{CO})_6$  alone, it tends to decrease slightly above 15  $\text{MWcm}^{-2}$  for the deposition from  $\text{Mo}(\text{CO})_6$  alone and from the mixture. SEM photographs show that the films from each carbonyl and their mixture consist of small grains that are more densely packed at higher beam intensities. The comparison of the film thickness evaluated from sputtering time to remove the films with that from direct observation with SEM suggests that the density of the film increases with beam intensity. In the films deposited from the mixture, molybdenum is preferentially incorporated from the gas phase. In addition, a model of gas-phase processes including photolysis of  $\text{Cr}(\text{CO})_6$ , transportation of photofragments to the substrate surface, and elimination of photofragments through chemical reactions during transportation, is proposed and simulated. Applications of the model will be discussed.

keywords: laser CVD, corrosion resistance,  $\text{Cr}(\text{CO})_6$ ,  $\text{Mo}(\text{CO})_6$

### Introduction

In recent years, numerous investigations have been carried out on the deposition of thin films from metal carbonyls using UV laser-induced chemical vapor deposition [1–6]. Although most of them have been conducted the practical application to the field of electro-optics and microelectronics, few studies have been carried out to improve corrosion resistance. In the present paper, we report a study on improving corrosion resistance of carbon steel by depositing chromium

and/or molybdenum from corresponding carbonyls using an ArF excimer laser (193nm). We prepared the films under different conditions and evaluate their corrosion resistance by an electrochemical method. Their microscopic structure, thickness and composition were also investigated and compared the corrosion resistance. A model of deposition processes is proposed and simulated calculations were done.

## Experimental

The setup for irradiation with an ArF excimer laser is shown in Fig.1.

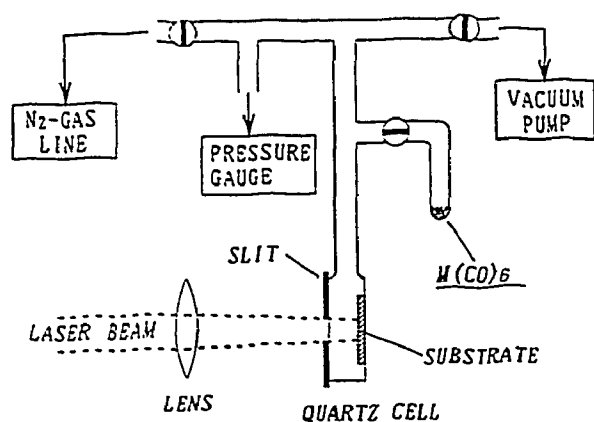


Fig.1 Experimental configuration for the deposition from metal carbonyls with an ArF excimer laser.

Carbonyls, Cr(CO)<sub>6</sub> and Mo(CO)<sub>6</sub> were used as received from Kojundo Kagaku. Carbon steel containing 0.14 atom% carbon purchased from KOBELCO. The excimer laser was Lambda Physik EMG 103, which was operated with 193 nm (ArF) under 10Hz.

The formed films were characterized by a scanning electron microscope (SEM), an Auger electron spectroscopy (AES) with 3 keV Ar<sup>+</sup> sputtering and an X-ray photoemission spectroscopy (XPS) with 0.6 keV Ar<sup>+</sup> sputtering. The corrosion resistance was evaluated by multi-sweep cyclic voltammetry in a 0.5M acetate buffer solution between the voltage of -700 and 300 mV (SCE) [7].

## Results and Discussion

### Microstructure (SEM)

The films showed similar structures, consisting of small grains with diameters smaller than 0.1μm. At higher beam intensities, the grains are more densely packed. Above the intensity of 20Mwcm<sup>-2</sup>, the surface structure is apparently changed. The surface is smoothed but cracks appeared. The film from Cr(CO)<sub>6</sub> alone are less significantly cracked than others at 25Mwcm<sup>-2</sup>. The smoothed surface corresponds to the metallic luster in appearance. SEM photographs of the film prepared by irradiation of the mixture of Cr(CO)<sub>6</sub> and Mo(CO)<sub>6</sub> with different intensities are shown in Figs. 2.

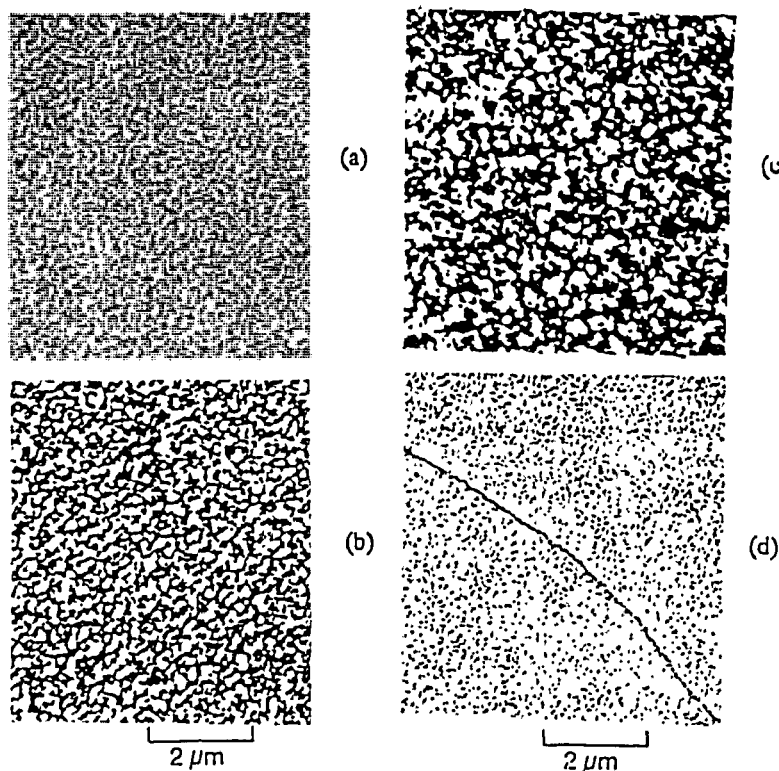


Fig.2 SEM photographs of the surface of the films deposited from the mixture of  $\text{Cr}(\text{CO})_5$  and  $\text{Mo}(\text{CO})_6$ . The films are obtained at beam intensities of (a)  $6 \text{ MW cm}^{-2}$ , (b)  $10 \text{ MW cm}^{-2}$ , (c)  $15 \text{ MW cm}^{-2}$  and (d)  $25 \text{ MW cm}^{-2}$ .

### Film Composition (AES & XPS)

In Fig.3, typical AES elemental depth profile of the film from the mixture of  $\text{Cr}(\text{CO})_5$  and  $\text{Mo}(\text{CO})_6$  at a beam intensity of  $15 \text{ MW cm}^{-2}$ .

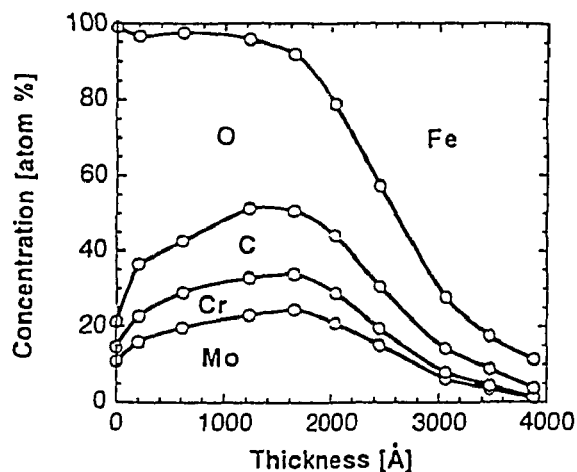


Fig.3 Typical AES elemental depth profile of the film deposited from the mixture of  $\text{Cr}(\text{CO})_5$  and  $\text{Mo}(\text{CO})_6$  at a beam intensity of  $15 \text{ MW cm}^{-2}$  and an irradiation time of 235 s.

The spectra of Cr from the film deposited from  $\text{Cr}(\text{CO})_5$  showed that chromium is oxidized at the surface while most of them exist as metal or carbide inside the surface. The chromium at the surface is likely to be oxidized by exposure to air after the deposition. The difference in binding energy between metallic Cr and  $\text{Cr}_3\text{C}_2$  is so small that the peaks were hardly discriminated the atomic ratio of the metal to the carbide in the inner layers is not clear because the accuracy in quantitative analysis is not enough. However, because the chromium at the surface is oxidized in air, it is likely that most of the chromium exists as metal. If most of the chromium originally existed as carbide, it would hardly be oxidized at the surface [8,9].

We could not obtain reliable information on the state of molybdenum inside the surface, because molybdenum oxide is readily reduced to metallic molybdenum by Ar<sup>+</sup> beam sputtering. We have checked the effect of the Ar<sup>+</sup> beam on the MoO<sub>3</sub> and Cr<sub>2</sub>O<sub>3</sub> layers on respective metals prepared by thermal oxidation. XPS spectra of Mo showed that irradiation with Ar<sup>+</sup> beam readily reduces MoO<sub>3</sub> and forms metallic Mo atoms. In contrast, the irradiation did not reduce Cr<sub>2</sub>O<sub>3</sub> significantly.

### Thickness: direct and indirect measurements

The film thickness evaluated from the sputtering time is shown in Fig.4 as a function of laser beam intensity, where the thickness was determined as the depth indicating that the sum of the metal elements is half maximum.

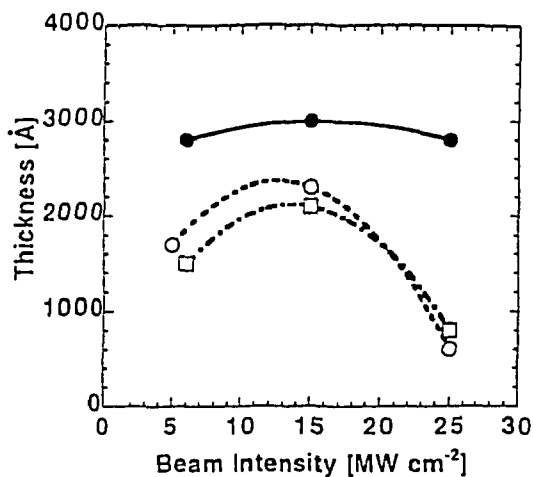


Fig.4 Film thickness evaluated from sectional view of the substrate observed with SEM. The open squares, open circles, and closed circles show the thickness from Cr(CO)<sub>6</sub>, Mo(CO)<sub>6</sub> and the mixture of Cr(CO)<sub>6</sub> and Mo(CO)<sub>6</sub> at an irradiation time of 235 s, respectively.

The thickness increases monotonically with beam intensity. On the contrary, the thickness evaluated from SEM also shown in Fig.4 shows a different dependence on beam intensity. The thickness of the film deposited from Cr(CO)<sub>6</sub> alone and Mo(CO)<sub>6</sub> alone increases with beam intensity up to an intensity of 15MWcm<sup>-2</sup>, decreasing above it. The thickness observed by SEM shows the actual thickness. It is likely that sputtering time corresponds to the amount of atoms deposited on the surface. This suggests that the density of the film increases with beam intensity, especially above 15MWcm<sup>-2</sup>,

which is consistent with the results on the surface microstructure that the grains are densely packed at higher intensities.

### Corrosion resistance: voltammetry

The initial peak current density for the carbon steel coated with the films from Cr(CO)<sub>6</sub> is shown as a function of beam intensity in Fig.5. Smaller current density shows higher corrosion resistance. The current density for uncoated carbon steel is about 20 mAcm<sup>-2</sup>. The current density is decreased by the coating with the film from Cr(CO)<sub>6</sub> shows the highest corrosion resistance over the beam intensities of 4 - 20 MWcm<sup>-2</sup>, and the corrosion resistance increases with beam intensity monotonically.

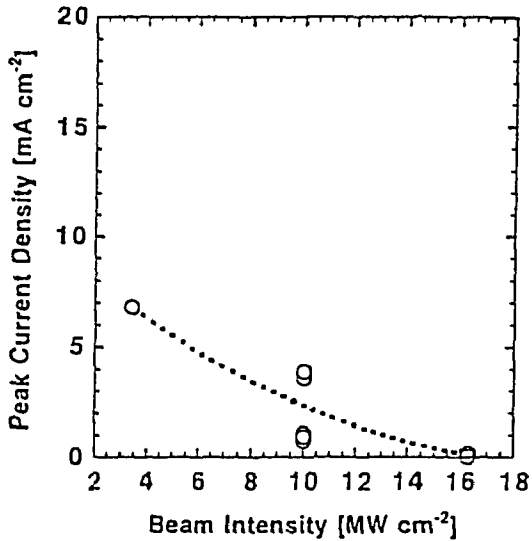


Fig.5 Dependence of the initial current density on beam intensity for the films formed from  $\text{Cr}(\text{CO})_6$  at irradiation of  $200 \text{ Jcm}^{-2}$ .

The carbon steel coated with the film from  $\text{Mo}(\text{CO})_6$  alone shows the lowest corrosion resistance. In addition, the corrosion resistance increases up to  $15 \text{ MWcm}^{-2}$ , while slightly decreases and scatters much above it. The resistance from the mixture gas lower than that from  $\text{Cr}(\text{CO})_6$ , while higher than that from  $\text{Mo}(\text{CO})_6$ . The scattering and slight decrease of the resistance at high intensities are also observed. It is likely that the increase of corrosion resistance with beam intensities is caused by the more densely packed, less porous film formation at higher intensities, suggested from the results on the microstructure and the thickness. The slight decrease at high intensities observed in the film of  $\text{Mo}(\text{CO})_6$  and the

mixture would be caused by the cracking that is more significant than that in the film deposited from  $\text{Cr}(\text{CO})_6$ .

### Modeling of gas phase processes

We have proposed a model for the deposition from  $\text{Cr}(\text{CO})_6$  induced by an excimer laser at low pressure on the basis of the chemical reactions in gas phase to describe the elimination of photofragments through reforming to  $\text{Cr}(\text{CO})_6$ .

#### Dissociation process

When the reactant molecules,  $\text{Cr}(\text{CO})_6$ , are decomposed by a single photon process, the concentration of  $\text{Cr}(\text{CO})_6$ ,  $R(t)$ , in a differential volume at time  $t$  is obtained by the equation

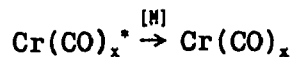
$$-dR(t)/dt dV = \sigma \phi I(t) R(t) dV$$

where  $\phi$  is the quantum yield of dissociation,  $\sigma$  is the absorption cross section,  $I(t)$  is the photon flux at time  $t$ .

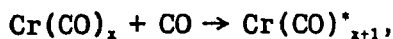
#### Recombination process

The fragments are classified into the excited state fragments,  $\text{Cr}(\text{CO})_x^*$  ( $x=0-6$ ), and the ground state fragments,  $\text{Cr}(\text{CO})_x$  ( $x=0-5$ ). Then the reforming process

in divided into the two stages: the stabilization reactions and the recombination reactions. Excited fragments are stabilized by collisions with buffer gases,



where  $x=0-6$ , M is the buffer gas representing Ar, CO,  $\text{Cr(CO)}_6$ , and the ground state fragments,  $\text{Cr(CO)}_x$  ( $x=0-5$ ). Subsequently, the ground-state fragments recombine with CO via recombination reaction



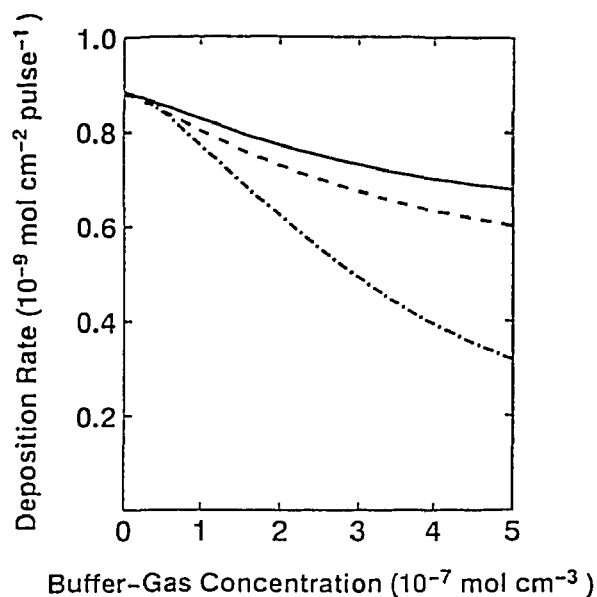
where  $x = 0-5$ .

We make a simple assumption that all kinds of the photofragments stick to the surface if they impinge on it. The coordinatively unsaturated species,  $\text{Cr(CO)}_x$  and  $\text{Cr(CO)}_x^*$  ( $x=0-5$ ), are expected to stick to the surface because they have free ligands to bind with the surface. The excited saturated fragments,  $\text{Cr(CO)}_6^*$ , are also expected to stick to the surface.

### Transportation

The transportation process of the fragments to the substrate surface depends on pressure. In the present study, the pressure region around 1 torr is of interest. This region is, unfortunately, a transition regime between ballistic and diffusive motion. The fragments arrive at the surface with 0-100 collisions depending on the distance from the surface and the transient pressure in the system. In order to avoid complicated treatments, we assume that the fragments move in ballistic motion.

### Simulation: Concentration and deposition rate [10]



The amount of molecules deposited per pulse is shown as the value after  $50 \mu\text{s}$ ,  $8.8 \times 10^{-10} \text{ mol cm}^{-2}$ , which is of the same order as an approximate experimental values in the present experiment,  $5 \times 10^{-10} \text{ mol cm}^{-2}$ , as shown in Fig.6.

Fig.6 Deposition rate as a function of buffer gas concentration. The solid line shows the dependence on Ar concentration in the absence of additional CO. The dashed line shows the dependence in the presence of additional CO of  $2 \times 10^{-8} \text{ mol cm}^{-3}$ . The dotted line shows the dependence of CO.

The results suggest that the deposition is initiated by photolysis in the gas phase and that the stabilization reactions play a significant role in the recombination process in the gas phase. The secondary process that follows condensation of the fragments on the surface is not included. More complete deposition models, including the secondary process, are required for a detailed discussion on the properties of the film such as film composition and dependence of the deposition on beam intensity.

Above results were published in a series of papers [10-12] and summarized elsewhere [13].

## References

- [1] D. Bäuerle: *Chemical Processing with Lasers*, Springer Ser. Mater. Sci., Vol.1 (Springer Berlin, Leidelberg 1986) pp.69-134.
- [2] N. S. Gluck, G. J. Wolga, C. E. Bartosch, W. Ho, Z. Ying; *J. Appl. Phys.*, **61**, 988 (1987)
- [3] R. L. Jackson, G. W. Tyndall, S. D. Sather; *Appl. Surf. Sci.*, **36**, 119 (1989)
- [4] K. A. Singmaster, F. A. Houle, R. J. Wilson: *Appl. Phys. Lett.*, **53**, 1048 (1988)
- [5] H. Yokoyama, F. Uesugi, S. Kishida, K. Washio; *Appl. Phys. A* **37**, 25 (1985)
- [6] R. Nowak, L. Konstantinov, P. Hess; *Matr. Res. Soc. Symp. Proc.*, **129**, 85 (1989)
- [7] U. R. Evans; *The Corrosion and Oxidation of Metals: Scientific Principles and Practical Applications* (Edward Arnold, London, 1960) pp.860-910
- [8] K. A. Singmaster, F. A. Houle, R. J. Wilson: *J. Phys. Chem.*, **94**, 6864 (1990)
- [9] R. Nowak, P. Hess, H. Oetzmann, C. Schmidt; *Appl. Surf. Sci.*, **43**, 11 (1989)
- [10] Used parameters and details of the procedure for calculation were shown in N. Okada, Y. Katsumura and K. Ishigure; *Appl. Phys. A* **56**, 138 (1993)
- [11] N. Okada, Y. Katsumura and K. Ishigure; *Appl. Phys. A* **55**, 207 (1992)
- [12] N. Okada, Y. Katsumura and K. Ishigure; *Appl. Phys. A* **58**, 99 (1994)
- [13] N. Okada (1993) Thesis, The University of Tokyo